The Developmental Brain Age Is Associated With Adversity, Depression, and Functional Outcomes Among Adolescents

Supplemental Information

Recruitment criteria, scanning protocols, and quality control protocols

Offspring of parents affected by mental illness were recruited via their parents' contact with the mental health services in Nova Scotia, Canada. Control offspring, matched for socioeconomic status and in similar age brackets were recruited through the local school board and through community organizations. One assessor conducted the cognitive assessment, another interviewed the parent(s). A third assessor performed the structured and semi structured interviews to assess youth psychopathology. Thus, parent assessors were blind to information on youth psychopathology and youth assessors were blind to information on parent psychopathology. Socioeconomic status (SES) was captured as a composite variable (range 0 to 5) indexing; 1) maternal and 2) paternal levels of education 3) family household annual income, 4) ownership of primary residence, and 5) ratio of bedrooms to residents in household, as previously described (1,2). Higher numeric value reflects higher SES.

Scans were processed with a modified Human Connectome Project (HCP) Minimal Preprocessing Pipeline (3). The HCP pipeline is a well-documented set of scripts developed to analyze high-quality multimodal MRI data. It leverages the most widely used open-source MRI processing software: FreeSurfer 6 (RRID:SCR_001847) and the FMRIB Software Library (FSL, RRID:SCR_002823). We have optimized the pipeline for

our data by matching it to our acquisition parameters and by replacing the MNI template with a pediatric template for registration. The modified pipeline is available and freely accessible at: https://github.com/GitDro/YouthReliability/tree/master/HCP_custom_pipeline.

We used the NIHPD pediatric atlas (NIHPD Objective 1 atlases [4.5–18.5 years], RRID:SCR_008794) to minimize registration bias in our developmental cohort.

Automated quality assurance was completed with the Qoala-T tool (4); Qoala-T website. Qoala-T is machine learning tool designed to automatically classify the quality of FreeSurfer output. All images in FORBOW were visually inspected by two independent raters and cross-referenced with Qoala-T automated results. There was substantial agreement for images rated for inclusion/exclusion by automated QC and human ratings (Chisq = 35.61, p=2.41e-09). In rare cases of disagreement between automated ratings and visual inspection we were conservative and excluded based on lowest rating from either method. For example, if Qoala-T recommended inclusion but raw inspection was rated as poor we discarded the scan. Human ratings for all external data were not feasible due to the overwhelming number of scans. External data with Qoala-T scores below 50 was excluded.

Supplemental Table S1. FORBOW cohort demographics.

	***n* (%)**
Female	79 (53 %)
Any adversity / disadvantage (PolyE > 0)	113 (75%)
Antecedents (YETI >= 8)	71 (47 %)
Lifetime MDD	24 (16 %)
Functional impairment (CIS >= 15)	22 (15%)
Family history of SMI	118 (68 %)
Lifetime Anxiety Disorder	63 (42 %)
Lifetime ADHD	37 (25 %)
Any cannabis use	15 (10 %)
Percent related	43 (29 %)
	Mean ± SD
Age	13.6 ± 2.8
FSIQ	106 ± 13.5
SES (0-5)	3 ± 1.42

PolyE = Polyenviromic Adversity Score. YETI = Youth Experience Tracker Instrument. MDD = Major Depressive Disorder. CIS = Columbia Impairment Scale. SMI = Severe Mental Illness. ADHD = Attention-deficit/hyperactivity disorder. FSIQ = Full-scale Intelligence Quotient. SES = Socioeconomic Status.

Supplemental Table S2. Scans across time points. The FORBOW study design includes short term reliability scans (weeks apart) as well as longitudinal follow up (months/years apart).

Scan time	N	Description
A	150	Baseline scan
B	49	Short term repeat of A
C	86	Longitudinal follow up 1
D	21	Short term repeat of C
E	24	Longitudinal follow up 2
F	3	Short term repeat of E
G	4	Longitudinal follow up 3
H	1	Short term repeat of G

Supplemental Table S3. List of features used in brain age model training and prediction.

FS_InterCranial_Vol	FS_BrainSeg_Vol	FS_BrainSeg_Vol_No_Vent
FS_BrainSeg_Vol_No_Vent_Surf	FS_LCort_GM_Vol	FS_RCort_GM_Vol
FS_TotCort_GM_Vol	FS_SubCort_GM_Vol	FS_Total_GM_Vol
FS_SupraTentorial_Vol	FS_SupraTentorial_Vol_No_Vent	FS_SupraTentorial_No_Vent_Voxel_Count
FS_Mask_Vol	FS_BrainSegVol_eTIV_Ratio	FS_MaskVol_eTIV_Ratio
FS_L_LatVent_Vol	FS_L_InfLatVent_Vol	FS_L_Cerebellum_WM_Vol
FS_L_Cerebellum_Cort_Vol	FS_L_ThalamusProper_Vol	FS_L_Caudate_Vol
FS_L_Putamen_Vol	FS_L_Pallidum_Vol	FS_3rdVent_Vol
FS_4thVent_Vol	FS_BrainStem_Vol	FS_L_Hippo_Vol
FS_L_Amygdala_Vol	FS_CSF_Vol	FS_L_AccumbensArea_Vol
FS_L_VentDC_Vol	FS_L_Vessel_Vol	FS_L_ChoroidPlexus_Vol
FS_R_LatVent_Vol	FS_R_InfLatVent_Vol	FS_R_Cerebellum_WM_Vol
FS_R_ThalamusProper_Vol	FS_R_Caudate_Vol	FS_R_Putamen_Vol
FS_R_Pallidum_Vol	FS_R_Hippo_Vol	FS_R_Amygdala_Vol
FS_R_AccumbensArea_Vol	FS_R_VentDC_Vol	FS_R_Vessel_Vol
FS_R_ChoroidPlexus_Vol	FS_OpticChiasm_Vol	FS_CC_Posterior_Vol
FS_CC_MidPosterior_Vol	FS_CC_Central_Vol	FS_CC_MidAnterior_Vol
FS_CC_Anterior_Vol	FS_L_Bankssts_Area	FS_L_Caudalanteriorcingulate_Area
FS_L_Caudalmiddlefrontal_Area	FS_L_Cuneus_Area	FS_L_Entorhinal_Area
FS_L_Fusiform_Area	FS_L_Inferiorparietal_Area	FS_L_Inferiortemporal_Area
FS_L_Isthmuscingulate_Area	FS_L_Lateraloccipital_Area	FS_L_Lateralorbitofrontal_Area
FS_L_Lingual_Area	FS_L_Medialorbitofrontal_Area	FS_L_Middletemporal_Area
FS_L_Parahippocampal_Area	FS_L_Paracentral_Area	FS_L_Parsopercularis_Area
FS_L_Parsorbitalis_Area	FS_L_Parstriangularis_Area	FS_L_Pericalcarine_Area
FS_L_Postcentral_Area	FS_L_Posteriorcingulate_Area	FS_L_Precentral_Area
FS_L_Precuneus_Area	FS_L_Rostralanteriorcingulate_Area	FS_L_Rostralmiddlefrontal_Area
FS_L_Superiorfrontal_Area	FS_L_Superiorparietal_Area	FS_L_Superiortemporal_Area

FS_L_Supramarginal_Area	FS_L_Frontalpole_Area	FS_L_Temporalpole_Area
FS_L_Transversetemporal_Area	FS_L_Insula_Area	FS_R_Bankssts_Area
FS_R_Caudalanteriorcingulate_Area	FS_R_Caudalmiddlefrontal_Area	FS_R_Cuneus_Area
FS_R_Entorhinal_Area	FS_R_Fusiform_Area	FS_R_Inferiorparietal_Area
FS_R_Inferiortemporal_Area	FS_R_Isthmuscingulate_Area	FS_R_Lateraloccipital_Area
FS_R_Lateralorbitofrontal_Area	FS_R_Lingual_Area	FS_R_Medialorbitofrontal_Area
FS_R_Middletemporal_Area	FS_R_Parahippocampal_Area	FS_R_Paracentral_Area
FS_R_Parsopercularis_Area	FS_R_Parsorbitalis_Area	FS_R_Parstriangularis_Area
FS_R_Pericalcarine_Area	FS_R_Postcentral_Area	FS_R_Posteriorcingulate_Area
FS_R_Precentral_Area	FS_R_Precuneus_Area	FS_R_Rostralanteriorcingulate_Area
FS_R_Rostralmiddlefrontal_Area	FS_R_Superiorfrontal_Area	FS_R_Superiorparietal_Area
FS_R_Superiortemporal_Area	FS_R_Supramarginal_Area	FS_R_Frontalpole_Area
FS_R_Temporalpole_Area	FS_R_Transversetemporal_Area	FS_R_Insula_Area
FS_L_Bankssts_GrayVol	FS_L_Caudalanteriorcingulate_GrayVol	FS_L_Caudalmiddlefrontal_GrayVol
FS_L_Cuneus_GrayVol	FS_L_Entorhinal_GrayVol	FS_L_Fusiform_GrayVol
FS_L_Inferiorparietal_GrayVol	FS_L_Inferiortemporal_GrayVol	FS_L_Isthmuscingulate_GrayVol
FS_L_Lateraloccipital_GrayVol	FS_L_Lateralorbitofrontal_GrayVol	FS_L_Lingual_GrayVol
FS_L_Medialorbitofrontal_GrayVol	FS_L_Middletemporal_GrayVol	FS_L_Parahippocampal_GrayVol
FS_L_Paracentral_GrayVol	FS_L_Parsopercularis_GrayVol	FS_L_Parsorbitalis_GrayVol
FS_L_Parstriangularis_GrayVol	FS_L_Pericalcarine_GrayVol	FS_L_Postcentral_GrayVol
FS_L_Posteriorcingulate_GrayVol	FS_L_Precentral_GrayVol	FS_L_Precuneus_GrayVol
FS_L_Rostralanteriorcingulate_GrayVol	FS_L_Rostralmiddlefrontal_GrayVol	FS_L_Superiorfrontal_GrayVol
FS_L_Superiorparietal_GrayVol	FS_L_Superiortemporal_GrayVol	FS_L_Supramarginal_GrayVol
FS_L_Frontalpole_GrayVol	FS_L_Temporalpole_GrayVol	FS_L_Transversetemporal_GrayVol
FS_L_Insula_GrayVol	FS_R_Bankssts_GrayVol	FS_R_Caudalanteriorcingulate_GrayVol

FS_R_Caudalmiddlefrontal_GrayVol	FS_R_Cuneus_GrayVol	FS_R_Entorhinal_GrayVol
FS_R_Fusiform_GrayVol	FS_R_Inferiorparietal_GrayVol	FS_R_Inferiortemporal_GrayVol
FS_R_Isthmuscingulate_GrayVol	FS_R_Lateraloccipital_GrayVol	FS_R_Lateralorbitofrontal_GrayVol
FS_R_Lingual_GrayVol	FS_R_Medialorbitofrontal_GrayVol	FS_R_Middletemporal_GrayVol
FS_R_Parahippocampal_GrayVol	FS_R_Paracentral_GrayVol	FS_R_Parsopercularis_GrayVol
FS_R_Parsorbitalis_GrayVol	FS_R_Parstriangularis_GrayVol	FS_R_Pericalcarine_GrayVol
FS_R_Postcentral_GrayVol	FS_R_Posteriorcingulate_GrayVol	FS_R_Precentral_GrayVol
FS_R_Precuneus_GrayVol	FS_R_Rostralanteriorcingulate_GrayVol	FS_R_Rostralmiddlefrontal_GrayVol
FS_R_Superiorfrontal_GrayVol	FS_R_Superiorparietal_GrayVol	FS_R_Superiortemporal_GrayVol
FS_R_Supramarginal_GrayVol	FS_R_Frontalpole_GrayVol	FS_R_Temporalpole_GrayVol
FS_R_Transversetemporal_GrayVol	FS_R_Insula_GrayVol	

Brain age prediction and bias correction

Using the tidymodels parsnip package, we set the XGBoost model to regression mode, with 1500 trees. We tuned the hyper-parameters tree_depth, min_n, loss_reduction, sample_size, mtry, and learn_rate (Supplemental Table S4) with grid search using latin hypercube sampling (size = 500). The method involves near-random sampling of parameter values from a distribution of all possible parameter values.

From the tuned cross validated results, we selected the best model using the “one standard-error rule” to balance model complexity and performance (5). Specifically, we picked the simplest model, in terms of tree depth, that is within one standard error of the model with the lowest MAE. The depth of the tree represents the degree of feature interaction and can lead to high non-linearity and variance (6). The best model was then finalized on the whole training set (Supplemental Table S5).

Variable/feature importance refers to techniques that assign a score/importance to the input features (in this case brain regions) based on their utility in predicting a target variable (chronological age). For xgboost the default metric to assess variable importance is gain, which computes the average gain across all splits a particular feature is used in. Gain is based on the decrease in entropy after a dataset is split on a feature, such as the precuneus for example. More information is provided here:
https://xgboost.readthedocs.io/en/latest/R-package/discoverYourData.html
https://koalaverse.github.io/vip/

Across regression methods there is a tendency for prediction bias towards the group mean (7). In the context of brain age studies this is seen as a slight age overestimation in younger participants and underestimation of predicted age in the older participants. To adjust this, we used a linear bias correction method proposed by prior research (7,8). We fit a linear regression model on the validation set: predicted_age $= \alpha + \beta_1(\text{scan\_age}) + error$. To attain a bias corrected prediction, we subtracted the intercept from the predicted age and then divided it by the slope. The slope and intercept are generalizable when applied to new data (9), thus we used these coefficients from the validation set to correct the bias in the test set without requiring any information about the independent test sample.

Validation set: As expected, the brain-age-gap was correlated with age, showing bias ($r(320) = -0.73$, $p < 0.001$). We assessed the relationship between the predicted age and the chronological age: predicted_age $= 6.41 + 0.55(\text{scan\_age}) + error$. As recommended in the literature, we subtracted the intercept from the predicted age and then divided it by the slope for bias correction. This procedure inflated the variance of the predicted age, increasing the MAE to 1.98, however it eliminated the correlation between the brain-age-gap and chronological age ($r(320) < 0.001$, $p = 1$).

Testing set (FORBOW): We used the coefficients from the validation set to bias correct the predicted age. After bias correction the MAE was 1.86 and the brain-age-gap did not significantly correlate with chronological age ($r(336) = -0.07$, $p = 0.2$).

Supplemental Table S4. Parsnip standardized parameter names with their matching names in the underlying xgboost engine. Engine default values in brackets. Table and additional documentation available on the tidymodels website.

parsnip	**xgboost**
tree_depth	max_depth (6)
trees	nrounds (15)
learn_rate	eta (0.3)
mtry	colsample_bytree (1)
min_n	min_child_weight (1)
loss_reduction	gamma (0)
sample_size	subsample (1)
stop_iter	early_stop

Supplemental Table S5. Parameters of top 10 best (lowest MAE) XGBoost models in cross-validation. The final model was selected by lowest tree depth within a standard error of best absolute performing model. Final model parameters in bold below.

mtry	min_n	Tree_depth	Learn_rate	Loss_reduction	Sample_size	MAE	Std_err
36	17	9	0.015337	1.610e-07	0.3169	1.523	0.008356
62	36	10	0.016105	2.353e-05	0.5631	1.523	0.008136
88	22	13	0.014384	5.690e-06	0.5778	1.525	0.008075
61	**12**	**6**	**0.013062**	**8.068e-04**	**0.4874**	**1.526**	**0.007807**
176	5	10	0.011077	9.034e+00	0.2078	1.528	0.008351
177	10	10	0.006773	3.157e-06	0.4177	1.530	0.007813
92	14	11	0.005258	3.304e-06	0.4001	1.535	0.008140
44	16	4	0.019228	3.387e-09	0.7696	1.535	0.008000
186	17	11	0.026158	1.057e-06	0.3057	1.535	0.008781

Supplemental Figure S1. Breakdown of Polyenviromic Adversity Score.

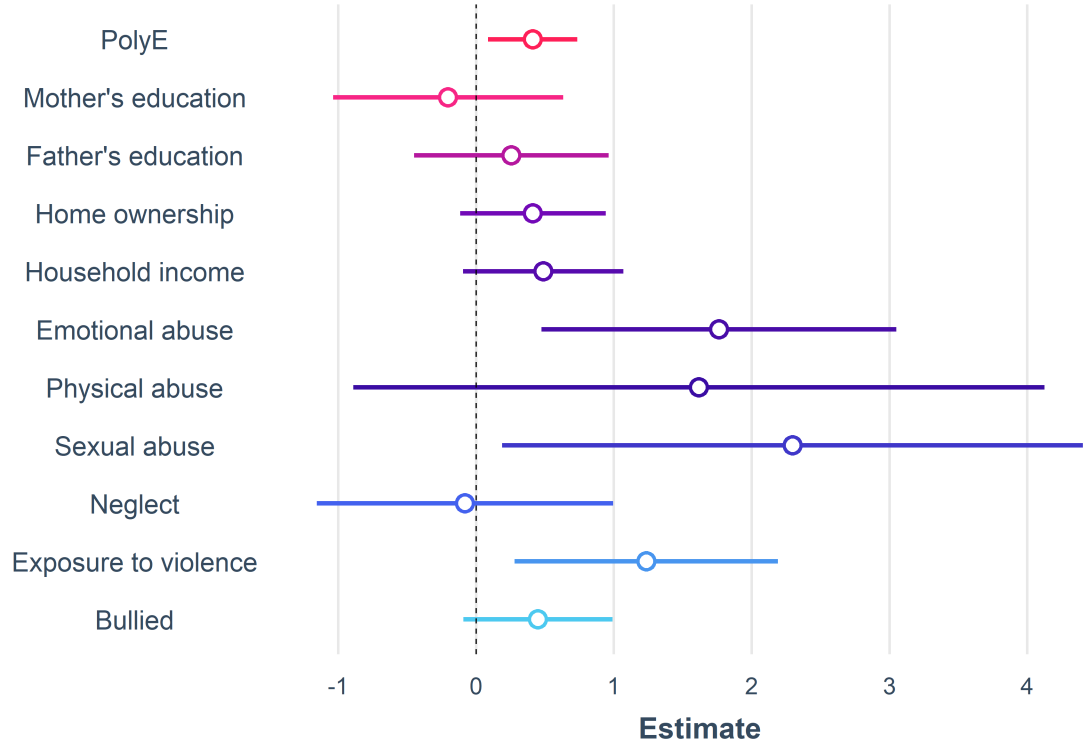

Breakdown of Polyenviromic (PolyE) adversity score. Most effects are in the direction of a positive brain-age-gap. Associations between adverse environments and a positive brain-age-gap are particularly strong for emotional abuse, sexual abuse, and exposure to violence in the home (see Supplemental Table S6 below).

Supplemental Table S6. Breakdown of Polyenviromic Adversity Score statistics summary.

	Est (β)	**2.5%**	**97.5%**	**t val.**	**p val.**
PolyE (Adversity)	0.18	0.04	0.31	2.42	**0.02**
Mother's education	-0.09	-0.44	0.27	-0.47	0.64
Father's education	0.11	-0.19	0.41	0.69	0.49
Home ownership status	0.18	-0.05	0.40	1.50	0.13
Annual household income	0.21	-0.04	0.46	1.61	0.11
Emotional abuse	0.75	0.20	1.29	2.61	**0.01**
Physical abuse	0.69	-0.38	1.75	1.22	0.22
Sexual abuse	0.97	0.08	1.87	2.06	**0.04**
Neglect	-0.03	-0.49	0.42	-0.14	0.89
Exposure to violence	0.52	0.12	0.93	2.46	**0.01**
Bullied	0.20	-0.04	0.44	1.60	0.11

Supplemental Figure S2. Multivariate models exploring the depression phenotype.

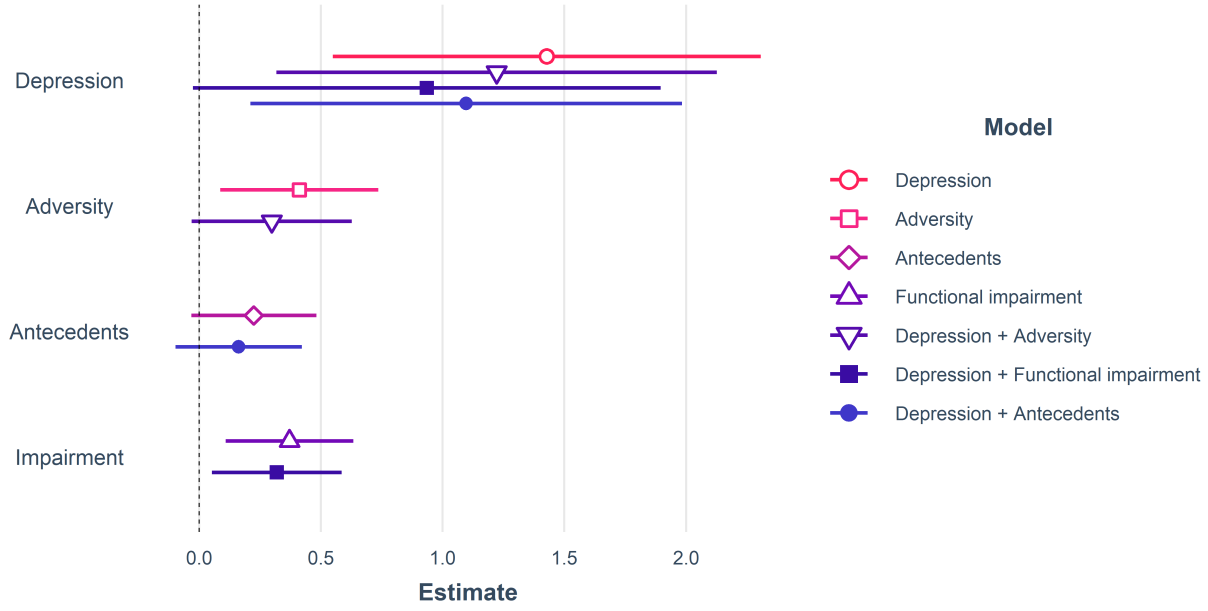

We wanted to explore the depression phenotype in the context of other factors from the main analysis which may be a risk for depression. To probe this question further we ran additional models with the brain-age-gap regressed on depression covarying for sex, age and importantly adversity, antecedents, and functional impairment. The exploratory models are plotted in Supplemental Figure S2, and statistical summaries are available in Supplemental Table S7.

While we lack the power to draw conclusive answers as these phenotypes are correlated and co-occur in many individuals, there are a few interesting effects worth noting. In a model containing depression and adversity, the effect size of adversity is reduced. In a model containing depression and functional impairment the effect of depression is reduced. However, given the high covariance between adversity, depression, and impairment, a much larger sample would be required to conclusively identify unique effects.

Supplemental Table S7. Statistical summary of main analysis and multivariate models.

Model	Predictor	Est (β)	2.5%	97.5%	t val.	p val.
Depression	Depression	0.61	0.23	0.99	3.12	**0.00**
Adversity	Adversity	0.18	0.04	0.31	2.42	**0.02**
Antecedents	Antecedents	0.10	-0.01	0.21	1.68	0.09
Impairment	Impairment	0.16	0.05	0.27	2.72	**0.01**
Depression + adversity	Depression	0.52	0.14	0.91	2.59	**0.01**
	Adversity	0.13	-0.01	0.27	1.73	0.09
Depression + impairment	Depression	0.40	-0.01	0.80	1.87	0.06
	Impairment	0.14	0.02	0.25	2.30	**0.02**
Depression + antecedents	Depression	0.48	0.09	0.88	2.37	**0.02**
	Antecedents	0.07	-0.04	0.19	1.20	0.23

Supplemental Figure S3. Results from the primary models and sensitivity analyses.

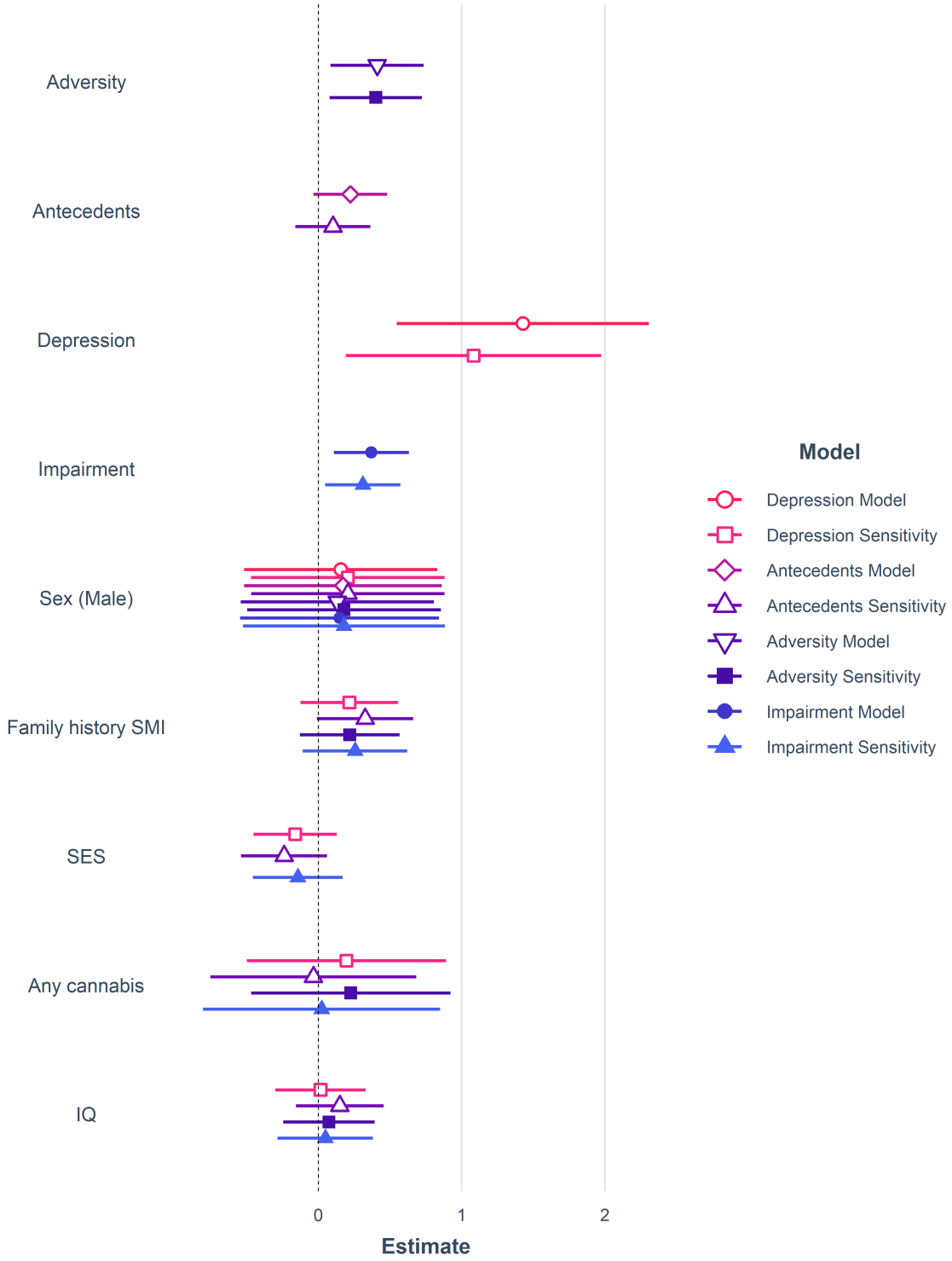

Supplemental References

1. MacKenzie LE, Patterson VC, Zwicker A, Drobinin V, Fisher HL, Abidi S, *et al.* (2017): Hot and cold executive functions in youth with psychotic symptoms. *Psychol Med* 47: 2844–2853.
2. Zwicker A, MacKenzie LE, Drobinin V, Bagher AM, Howes Vallis E, Propper L, *et al.* (2020): Neurodevelopmental and genetic determinants of exposure to adversity among youth at risk for mental illness. *J Child Psychol Psychiatry* 61: 536–544.
3. Glasser MF, Sotiropoulos SN, Wilson JA, Coalson TS, Fischl B, Andersson JL, *et al.* (2013): The minimal preprocessing pipelines for the Human Connectome Project. *Neuroimage* 80: 105–124.
4. Klapwijk ET, van de Kamp F, van der Meulen M, Peters S, Wierenga LM (2019): Qoala-T: A supervised-learning tool for quality control of FreeSurfer segmented MRI data. *Neuroimage* 189: 116–129.
5. Breiman L, Friedman J, Stone CJ, Olshen RA (1984): *Classification and Regression Trees*. CRC press.
6. James G, Witten D, Hastie T, Tibshirani R (2013): *An Introduction to Statistical Learning: With Applications in R*. Springer, New York, NY.
7. Smith SM, Vidaurre D, Alfaro-Almagro F, Nichols TE, Miller KL (2019): Estimation of brain age delta from brain imaging. *Neuroimage* 200: 528–539.
8. de Lange A-MG, Cole JH (2020, February 24): Commentary: Correction procedures in brain-age prediction. *NeuroImage. Clinical*, vol. 26. p 102229.

9. Peng H, Gong W, Beckmann CF, Vedaldi A, Smith SM (2020, November 6): Accurate brain age prediction with lightweight deep neural networks. *Cold Spring Harbor Laboratory*. p 2019.12.17.879346.